crystals

MDPI

*Review*

# Recent Developments of Carbon-Based Anode Materials for Flexible Lithium-Ion Batteries

**Ling Deng [1,2,3], Tongye Wei [1,*], Jie Liu [1], Li Zhan [1], Wei Chen [1] and Juexian Cao [1,2,*]**

[1] Hunan Institute of Advanced Sensing and Information Technology, Xiangtan University, Xiangtan 411105, China
[2] School of Physics and Optoelectronics, Xiangtan University, Xiangtan 411105, China
[3] School of Energy and Electromechanical Engineering, Hunan University of Humanities, Science and Technology, Loudi 417000, China
* Correspondence: weity@xtu.edu.cn (T.W.); jxcao@xtu.edu.cn (J.C.)

**Abstract:** Flexible lithium-ion batteries (FLIBs) have rapidly developed as promising energy storage devices for flexible and wearable electronics, owning to the advantages of high energy density, fast charge–discharge, no memory effect and stable cycle performance. Research on flexible electrodes has attracted widespread attention to maintain stable electrochemical function under deformation. Carbon materials are some of the most popular lithium-ion battery (LIB) anode materials owing to their low cost, high conductivity and excellent stability. However, the scaled-up fabrication of flexible electrodes based on carbon-based materials for high-performance FLIBs is still challenging. Herein, the fabrication strategies for FLIBs based on carbon materials such as carbon nanofibers (CNFs), carbon nanotubes (CNTs), graphene, graphdiyne (GDY) and carbon aerogels (CAs) are reviewed in terms of macroscopic electrode material preparation, property optimization and structure design. Furthermore, fabrication strategies and structure design methods for electrodes are proposed to improve energy capacity, cycle stability, conductivity and flexibility of FLIBs. This minireview can offer potential directions for the novel design of flexible carbon-based anodes employed in FLIBs.

**Keywords:** lithium-ion batteries; anode; flexibility; carbon materials; wearable electronics



**Citation:** Deng, L.; Wei, T.; Liu, J.; Zhan, L.; Chen, W.; Cao, J. Recent Developments of Carbon-Based Anode Materials for Flexible Lithium-Ion Batteries. *Crystals* **2022**, *12*, 1279. https://doi.org/10.3390/cryst12091279

Academic Editor: Yutaka Moritomo

Received: 27 July 2022
Accepted: 7 September 2022
Published: 9 September 2022



## 1. Introduction

The ever-increasing boom in flexible and wearable electronics, such as communication equipment, roll-up displays, smart garments and implantable medical devices, has triggered extensive efforts to develop matching energy storage devices. Among them, rechargeable LIBs have been widely recommended as ideal candidates for the advantage of high energy and power density, stable cycle performance and no memory effects [1]. The electrodes of conventional LIBs are generally fabricated by coating slurry with active materials, binders and conductive materials on the surface of current collectors, such as aluminum foils and copper foils. However, metal foils are heavy and low elastic limits and poor adhesion with active materials, which lead to insufficiently flexible and lightweight LIBs. Once deformation applied to the battery goes beyond the limit, fatal damage of the structure and recession of the electrochemical function may take place, and it fails to work.

As portable and wearable devices call for flexibility of batteries, conventional LIBs cannot satisfy the requirement. FLIBs share the same components (anode, cathode and electrolyte) and working mechanism as conventional LIBs. In addition, they also have some new features such as being foldable, stretchable, lightweight and implantable. Among all the components, electrodes are regarded as the core elements dominating the performance of LIBs. For the sake of exploring high-performance FLIBs, it is critical to develop flexible electrodes with high conductivity, outstanding mechanical flexibility and stable electrochemical performance under frequent and large deformation. To date, the fundamental way is to develop flexible freestanding electrodes free of binders, current collectors and

conductive materials, but that can be used as anodes or cathodes directly. For LIBs, anode materials can be carbon-based materials, silicon-based materials and metals and their oxides/nitrides/phosphides/sulfides.

Recently, carbon materials, such as 1-dimensional (1D): carbon nanotubes (CNTs), carbon nanofibers (CNFs); 2D: graphene, graphdiyne (GDY); and 3D: carbon foams (CFs), carbon aerogels (CAs), have attracted increasing interest in developing freestanding electrodes for flexible energy storage devices. In application, 2D paper-like batteries, interdigital electrode batteries, stretchable batteries and 1D fiber-shaped batteries are widely explored from the carbon materials mentioned above, as shown in Figure 1. In this minireview, we first investigated the most recent achievements devoted to carbon-based anode materials in preparation, structure and property; then highlighted their achievements in various types of FLIBs with emphasis on ingenious structure design and performance optimization. In the last section, for the sake of providing certain helpful insights for the continued development, major challenges, prospects and opportunities of carbon materials for FLIBs are discussed.

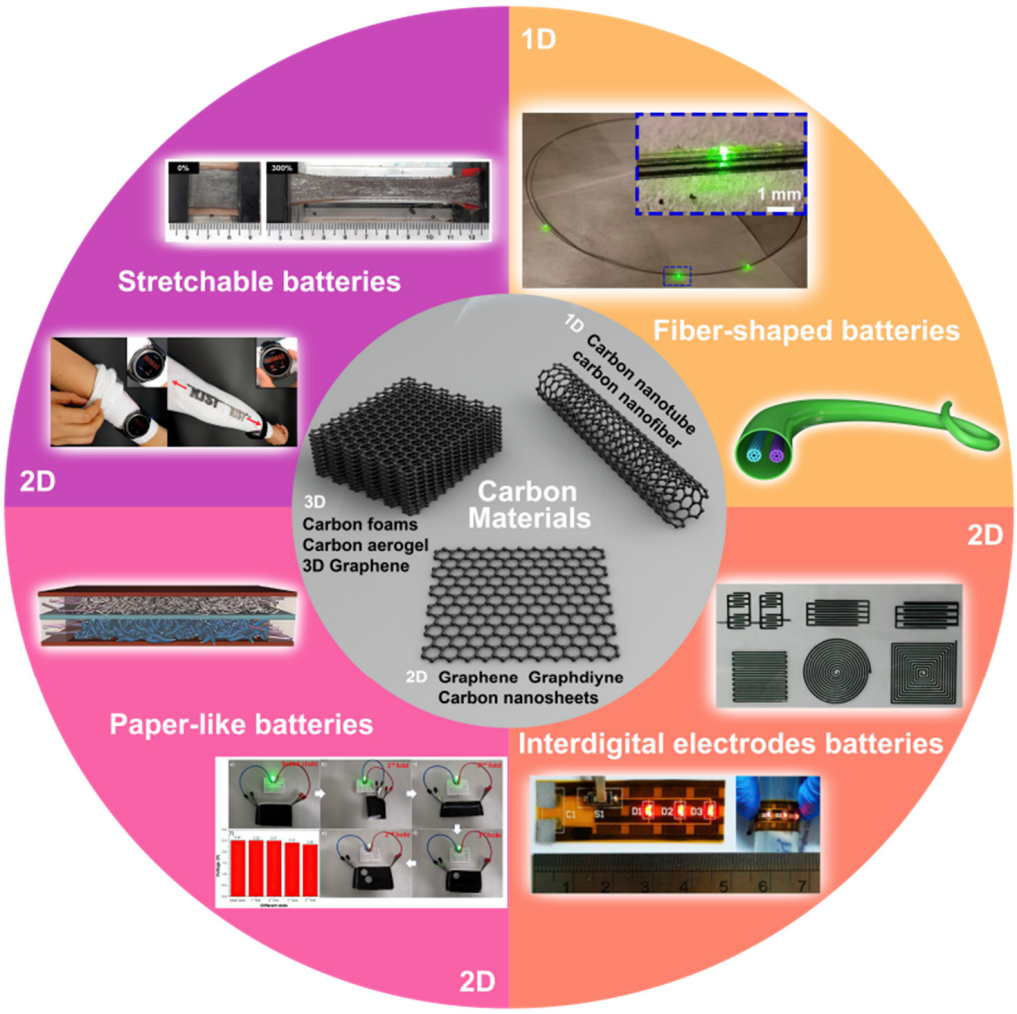


**Figure 1.** Schematic diagram of carbon materials and their application in FLIBs.

## 2. Carbon Materials

Carbon materials are preferred and practical electrode materials for energy storage devices for the advantages of light weight, low electrode potential, high conductivity and outstanding mechanical flexibility [1–3]. The materials with nanoscale dimensions and porous structure can effectively shorten the diffusion path of charged ions and increase the capacity by providing sufficient active sites. In addition, the low dimensional structure

plays a significant role in enhancing the structural stability. During the past decades, considerable studies have been carried out in order to prepare carbon materials, optimize structures and enhance performance. The most recent achievements in micromorphology, mechanical and electrochemical performance of carbon-based macroscopic materials for FLIBs in different dimensions will be discussed in detail.

### *2.1. 1D Carbon Materials*

As representative of one-dimensional materials, CNTs and CNFs have fast electron and ion transport features owing to their uniquely low dimensional structure. In addition, they can restrain the volume changes of active materials in the cycle and reduce the pulverization and agglomeration of materials.

In 1991, Iijima first synthesized CNTs using arc-discharge evaporation [4]. CNTs revealed a distinct 1D tubular structure composed of carbon atoms. According to the number of rolling graphene sheets, CNTs are divided into single-walled CNTs (SWCNTs) and multi-walled CNTs (MWCNTs) [5,6]. The property of CNTs depends on the arrangement of carbon atoms, tube diameter, length and shape state. SWCNTs are composed of only one graphene sheet layer, and their diameters are around 0.8 to 2 nm. Nanotubes formed with two or more graphene layers are called MWCNTs. The 0.34 nm gap between layers of MWCNTs can accommodate lithium ions. The capacity is linear to the diameter of the wall owing to lithium condensation reactions. According to the orientation of the carbon hexagon along the axial direction, also named chirality, SWCNTs are divided into three types: zigzag, armchair and chiral. The structure of SWCNTs determines their property and application. Zhao et al. found that the diffusion barriers of lithium increase with the increase in tube diameter [7]. In addition, CNTs have excellent mechanical behavior (Young's modulus and tensile strength of CNTs are reported to be up to 1.4 TPa and 500 GPa, respectively), large aspect ratio, high conductivity (400,000 S $cm^{-1}$) and high theoretical capacity (the reversible capacities for SWCNTs and MWCNTs are around 300–600 mAh $g^{-1}$, 1000 mAh $g^{-1}$, respectively), which also contribute to their application.

For building composite electrodes, CNTs are usually deposited or embedded on flexible substrates [8–12]. However, because of their large aspect ratio and remarkable flexibility, CNTs are prone to differ in length, agglomerate and become entangled in a freely growing environment, which badly limits their potential applications. Recently, Yang et al. made CNTs symmetrically grow on FeSiAl microflakes using rotating chemical vapor deposition (CVD) [13]. The high-purity array CNTs provided uniform structure and orientation and larger contact area (Figure 2a,b). In addition, they showed ideal application prospects for electrode materials.

CNTs have been demonstrated as promising flexible electrodes. Wang et al. prepared coaxial PANI@$SnO_2$@MWCNT composite (Figure 2c,d) by self-assembling $SnO_2$ nanoparticles on the surface of MWCNTs, then in situ coating PANI [14]. As a result, the as-fabricated electrodes exhibited outstanding rate capability and stable cycling performance for FLIBs. Guo et al. developed a CNT-based film decorated with $Ni_xCo_y$-silicate nanosheets [15]. The as-assembled composite film was sufficient to withstand various deformations because of its excellent flexibility. In addition, it showed excellent electrochemical performance with specific capacity as high as 1047 mAh $g^{-1}$ at the current density of 0.1 A $g^{-1}$ and capacity retention of 78.13% after 140 cycles.

CNFs have similar physical and electrochemical properties to CNTs and are ideal for Li-ion diffusion. The common and economical fabrication method of CNFs is electrospinning and follows carbonization [16–23]. Yu et al. prepared poly nanofibrous arrays in random (Figure 2e) and aligned (Figure 2f) orientations on glass slips [24]. Interestingly, the porous CNFs showed higher lithium storage capacity (435–600 mAh $g^{-1}$) than graphite. To introduce porosity into CNFs, blending carbon-generating materials and sacrificial polymers which decompose during carbonization at high temperature by the electrospinning technique has become a popular means. Li et al. prepared hierarchically porous CNFs (HPCNFs) with the use of poly and terephthalic acid [25], as shown in

Figure 2g–i. The specific capacitance and area capacitance for HPCNFs were up to 327 F $g^{-1}$ and 80.5 mF $cm^{-2}$, respectively.

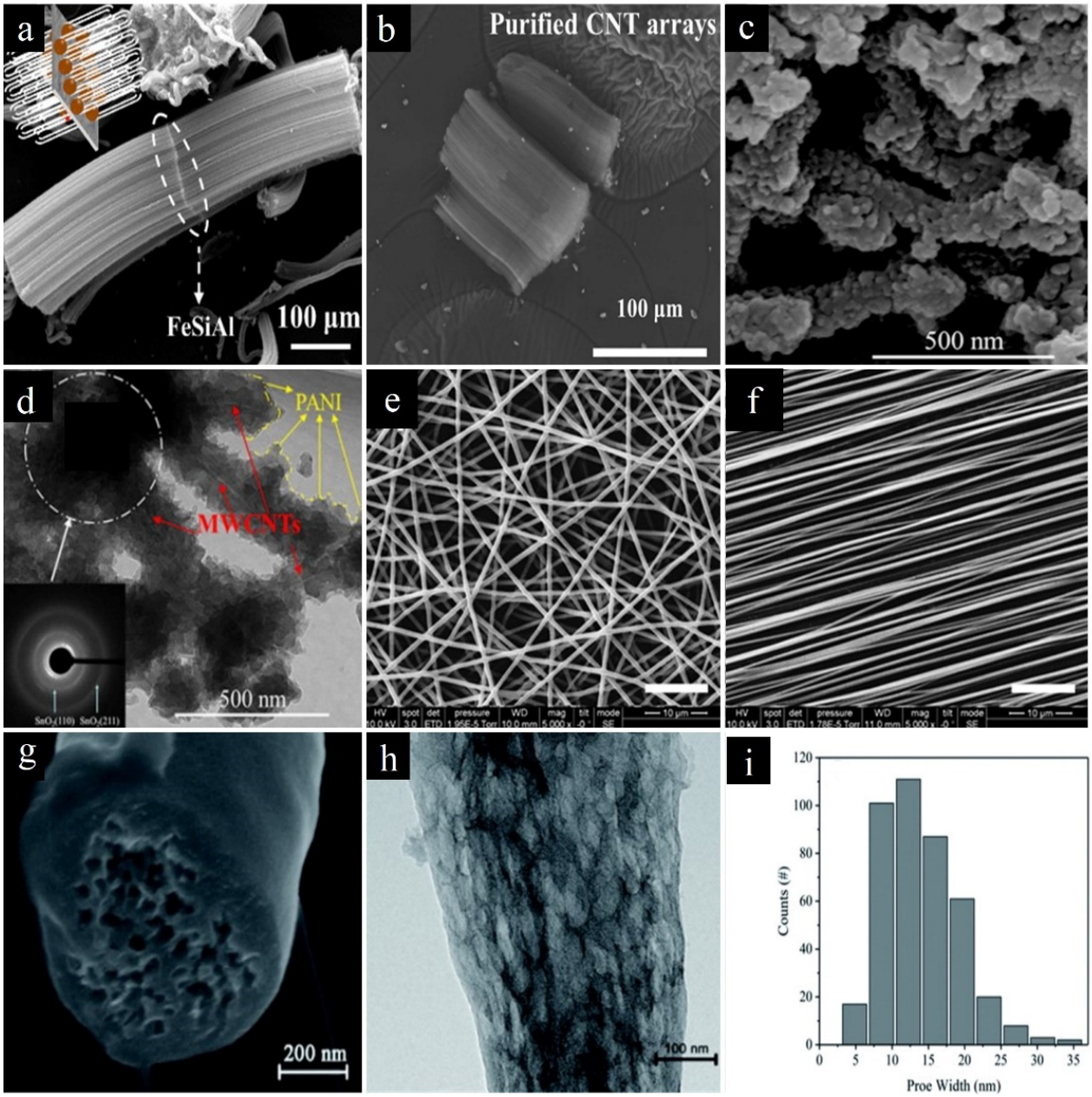


**Figure 2.** SEM images of CNT array (**a**) grown for 1 h at 700 °C; (**b**) after purification. (**a**,**b**) Reprinted with permission from [13]. Copyright Elsevier Publisher, 2022. (**c**,**d**) SEM and TEM images of PANI@$SnO_2$@MWCNTs. (**c**,**d**) Reprinted with permission from [14]. Copyright Elsevier Publisher, 2018. SEM images of PLGA nanofiber arrays in (**e**) random; (**f**) aligned orientations. (**e**,**f**) Reprinted with permission from [24]. Copyright Springer Nature Publisher, 2019. (**g**–**i**) SEM and HRTEM images and statistical histograms of the mesopore size for HPCNFs. (**g**–**i**) Reprinted with permission from [25]. Copyright Society of Chemistry Publisher, 2020.

### *2.2. 2D Carbon Materials*

As electrode materials, there are some unique advantages for 2D carbon materials, such as graphene (graphene oxide (GO) and reduced GO), graphdiyne (GDY) and carbon nanosheets. (1) Sufficient active sites are created on the edges of a large surface area (graphene, 2630 $m^2$ $g^{-1}$), which increase energy storage capacity. (2) Layered structure

with space between layers provides convenient diffusion pathways for charged ions, which promises high ionic conductivity (graphene, up to $10^6$ S $cm^{-1}$). Graphene, as a representative of 2D carbon materials, is very popular in practical applications [26–28]. The recent advancements in preparation, merits and applications of the corresponding macroscopic materials based on 2D carbon materials, especially graphene, are summarized in detail.

Graphene was first isolated by mechanical exfoliation with Scotch tape. For further application, a variety of rational synthesis routes have been developed, such as CVD, ball-milling and chemical oxidation-reduction of graphite [1,29]. Notably, different preparation strategies are prone to gain graphene with distinguished morphologies and properties. For example, the layers and defects of graphene are controllable in CVD through adjusting parameters, such as time and temperature, while this is impossible for the oxidation-exfoliation-reduction method. Scaled-up preparation of graphene with excellent quality and industrial fabrication of macroscopic materials with uniform morphologies and properties, such as fiber and film, are critical for the application.

Graphene fiber, mostly prepared by wet-spinning of homogeneous GO solution and further hydrothermal or chemical reduction, is a macroscopic carbon-based fiber with superior mechanical and electrochemical performance, such as light weight, excellent flexibility and ease of functionalization. At a constant concentration, the prearrangement orientation of large GO is more obvious, which gives graphene fiber high strength and modulus. Moreover, the large GO with fewer layer nodes and defects is conducive to improving the mechanical properties of the fiber. As shown in Figure 3a,b, Tang et al. produced graphene fibers by scalable additive-free wet-spinning methodology [30]. By optimizing the surface chemistry of GO sheets and controlling their spinning and fabrication behavior, the pristine fibers exhibited outstanding tensile strength (875.9 MPa), high toughness (13.3 MJ $m^{-3}$) and superb conductivity ($1.06 \times 10^5$ S $m^{-1}$). Zheng et al. prepared robust ultralight graphene fibers with hierarchical structure by a twist-spinning assembly strategy followed by chemical reduction and thermal treatment. All these property parameters mentioned above prove that graphene fiber is especially suitable for flexible electrodes of energy storage devices.

Based on the monolayer atomic structure, a graphene sheet, also named graphene paper, is expected to expand to the macrodimension. Asif Mahmood et al. synthesized freestanding graphene film with highly porous structure by temperature-dependent X-ray diffraction [31]. In addition, the overall interlayer spacing of 0.38–0.39 nm provided a fast mass transport pathway and allowed expansion/contraction of crystallite upon reversible ion intercalation. Liu et al. prepared hybrid films composed of hierarchical $Fe_{1-x}S$-filled porous carbon nanowires/rGO ($Fe_{1-x}S$@PCNWs/rGO) by facile assembly followed by sulfuration [32]. The as-fabricated film had a smooth surface and exhibited excellent mechanical deformation when bending, rolling, twisting and folding were evaluated in detail (Figure 3c).

GDY, a new promising allotrope of graphene, was first synthesized in 2010 by Li's group [33]. Its unique structure and property are beneficial for the rapid transmission of lithium ions with theoretical specific capacity as high as 744 mAh $g^{-1}$ [34]. There are some synthesis strategies of GDY and its derivatives, such as coupling reaction, solvothermal reaction and CVD. The morphology and size of GDY and its derivatives can be controlled and adjusted by changing the reaction conditions. To improve its performance, functionalization strategies, such as heteroatomic doping, are often employed [35]. Yang et al. successfully prepared novel pyrimidine-GDY and pyridine-GDY films [36]. As shown in Figure 3d, the film was deformable, freestanding and uniform. As an anode for FLIB, the film exhibited superior rate capability (Figure 2e) and long-term cycling performance (4000 cycles at 5 A $g^{-1}$) (Figure 2f).

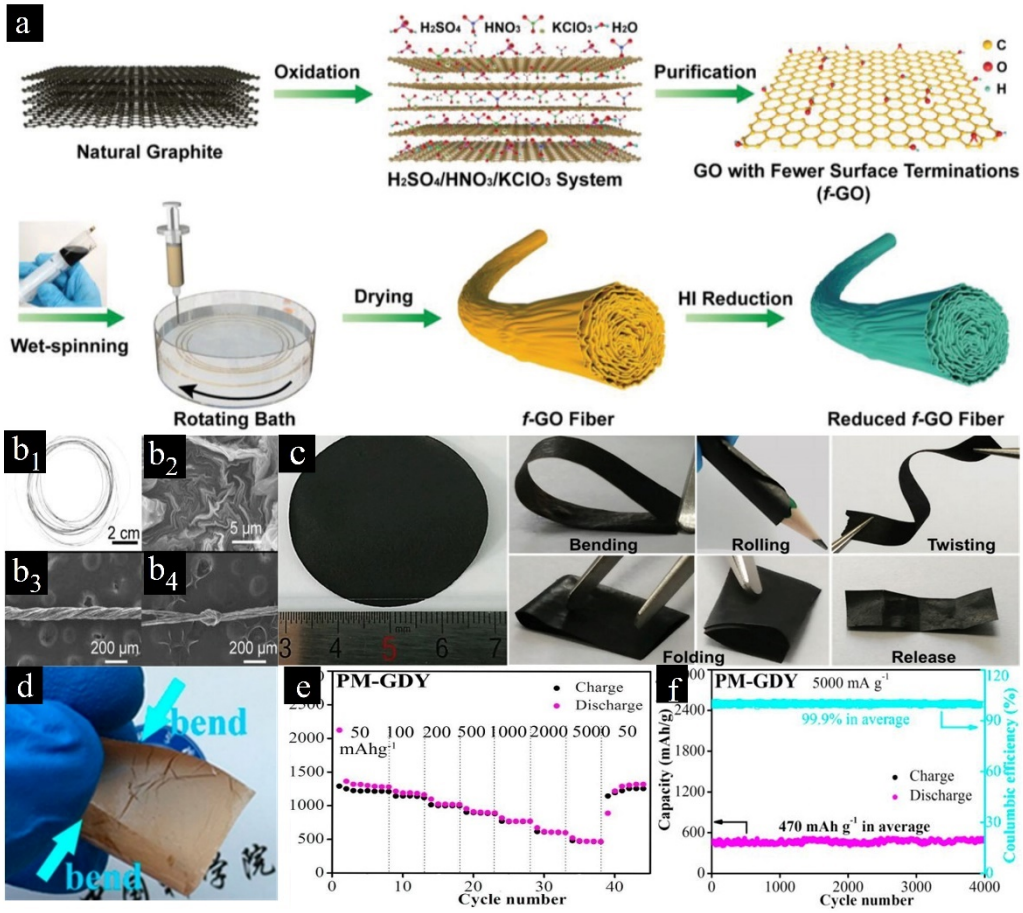


**Figure 3.** (**a**) Schematic of f-GO, (reduced)-GO fiber. Morphology and structure of f-GO fibers: (**b1**) Image of a 5 m fiber; SEM images of (**b2**) the fiber cross-section; (**b3**) twisted fibers and (**b4**) a tied fiber knot. (**a**,**b**) Reprinted with permission from [30]. Copyright John Wiley Publisher, 2022. (**c**) The appearance and flexibility exhibition images of the composite $Fe_{1-x}S$@PCNWs/rGO film. Reprinted with permission from [32]. Copyright John Wiley and Sons Publisher, 2019. (**d**) Image of the bending pyridine-GDY film. (**e**) Rate capacity and (**f**) Cycling performances of pyrimidine-GDY. (**d**–**f**) Reprinted with permission from [36]. Copyright American Chemical Society Publisher, 2019.

### *2.3. 3D Carbon Materials*

The 3D carbon materials, such as CFs and CAs, are composed of graphene and CNTs. The mutually cross-linked network with abundant pores exhibits high specific area and largely avoids an irreversible capacity loss. They are typical current collectors of anodes for FLIBs with high energy density. Yang et al. successfully fabricated lightweight and freestanding electrodes by blending CFs with SnS nanosheets [37]. They maintained high reversible capacity (747 mAh $g^{-1}$ after 100 cycles) and excellent rate capability in FLIBs. The facile preparation of CFs is to carbonize various carbon-based precursors, such as polymers and pitches. Shi et al. obtained freestanding porous CFs by pyrolyzing commercial melamine foam at 900 °C under a nitrogen atmosphere (Figure 4a) [6]. As shown in Figure 4b, the uniformly distributed and interconnected pores in CFs acted as reservoirs for electrolytes, which were conducive to ion diffusion. The CF block recovered its original structure and size when unloaded, which exhibited its excellent deformability (Figure 4c).

CAs are synthetic gels with porous non-shrinking network structure and gas occupies 90−99% of the whole volume [38,39]. Owing to their ultralow density, abundant porosity, multi-functionality and excellent electrical conductivity, CAs are usually employed as electrodes with high capacity and excellent cycle stability for energy storage devices,

such as rechargeable batteries and supercapacitors. The preparation of CAs includes three steps, i.e., polymerization, drying and carbonization [40]. Researchers found that the facile preparation of CAs can be realized by selecting the appropriate precursors and preparation conditions [41–48]. By hierarchical synergistic assembly, Guo et al. reported highly stretchable neat CAs prepared by ink-printing a uniform mixture of GO and MWCNTs, followed by freeze-drying and further reduction (Figure 4d) [49]. The CAs are extremely lightweight and can be supported by a flower (Figure 4e). They were fabricated to various orders of structural hierarchy spanning from centimeter to molecular scale (Figure 4f–i). In addition, the programmed direct writing made the design of bending dominated macrolattices control tensile behaviors and Poisson ratios, for example, the honeycomb with a negative Poisson ratio in Figure 4j, positive in Figure 4k and zero in Figure 4l. The expansion rate of the structure could reach 200%, which indicated they were suitable for stretchable and flexible energy storage devices.

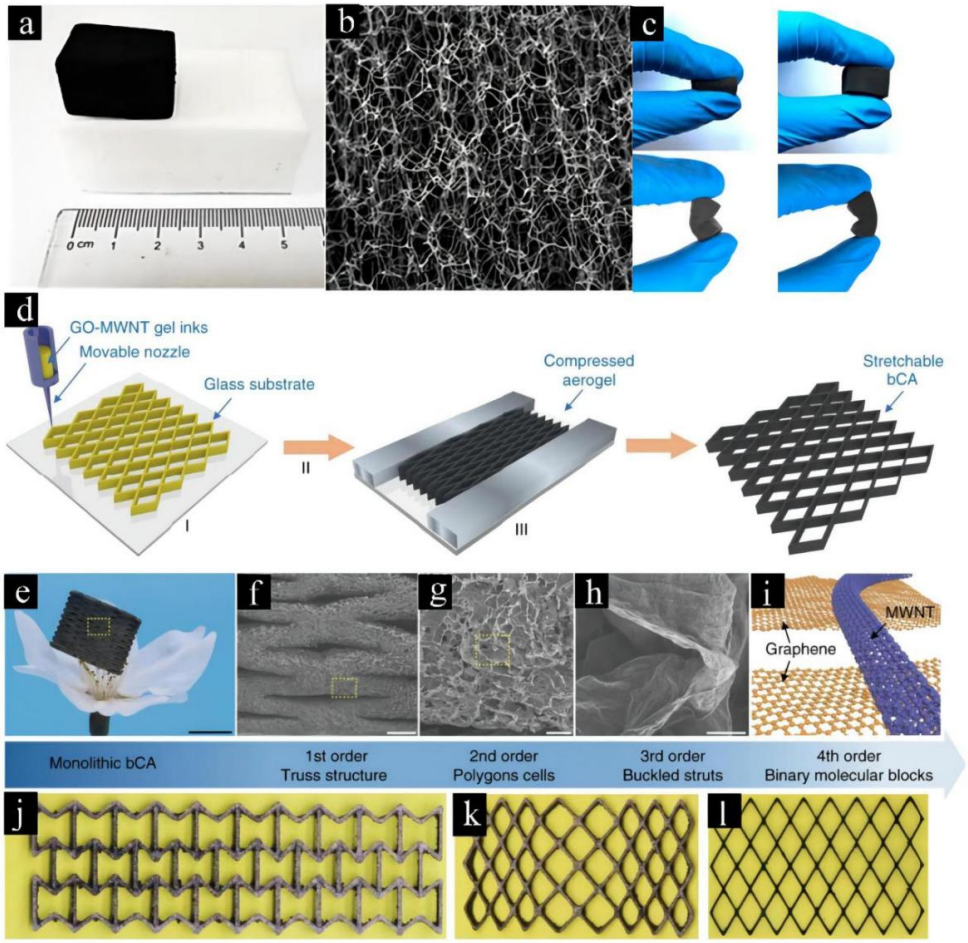


**Figure 4.** (**a**) Image of melamine foam and CF. (**b**) FESEM image of the CF. (**c**) CF compressed and bent by finger. (**a**–**c**) Reprinted with permission from [6]. Copyright Elsevier Publisher, 2021. (**d**) Schematic of the CA assembly by 3D printing (I), freeze-drying (II) and reduction (III). (**e**) Image of CA balancing on a flower. (**f**–**i**) SEM images of CAs in various size scales. (**j**–**l**) Printed structures with negative (−0.3, (**g**)), positive (+0.5, (**h**)) and zero Poisson ratio (0, (**l**)). Scale bars, 5 mm (**e**), 500 μm (**f**), 100 μm (**g**) and 5 μm (**h**). (**d**–**l**) Reprinted with permission from [49]. Copyright Springer Nature Publisher, 2018.

## 3. Application in Flexible Lithium-Ion Batteries

With the rapid propagation of technology, wearable and implantable electronics have stimulated the unprecedented development of microscopic and flexible energy storage devices. Among them, FLIBs emerge as the most promising candidates owing to their high

energy density and stable cycle performance. Flexible electrodes, as the central complement of FLIBs, have attracted widespread attention from researchers for developing electrodes with excellent electrochemical performance and mechanical stability. Recently, flexible freestanding electrodes based on carbon materials have been widely investigated, so as to exploit outstanding FLIBs with 1D and 2D structures.

### *3.1. 1D Fiber-Shaped Batteries*

The fiber-shaped battery was first developed by ITN Energy Systems for assembling a planar battery with fiber electrodes in 2011 [50]. Recently, Khudiyev et al. presented an ultralong Li-ion fiber battery by the thermal drawing method [51], as shown in Figure 5. The continuous fiber-shaped battery with a length of 140 m demonstrated discharge capacity as high as 123 mAh and discharge energy up to 217 mWh. The fiber-shaped batteries offer potential advantages. Firstly, they are ultralight and flexible enough to adapt to complex deformation, such as winding, twisting and tying. In addition, they have close contact with irregular surfaces. Secondly, the textiles fabricated with fiber-shaped batteries provide porous large surface structure and they are breathable. The 1D batteries, with omnidirectional flexibility, deformation adaptability and high compatibility with textiles, are excellent competitors of power supplies for practical wearable devices.

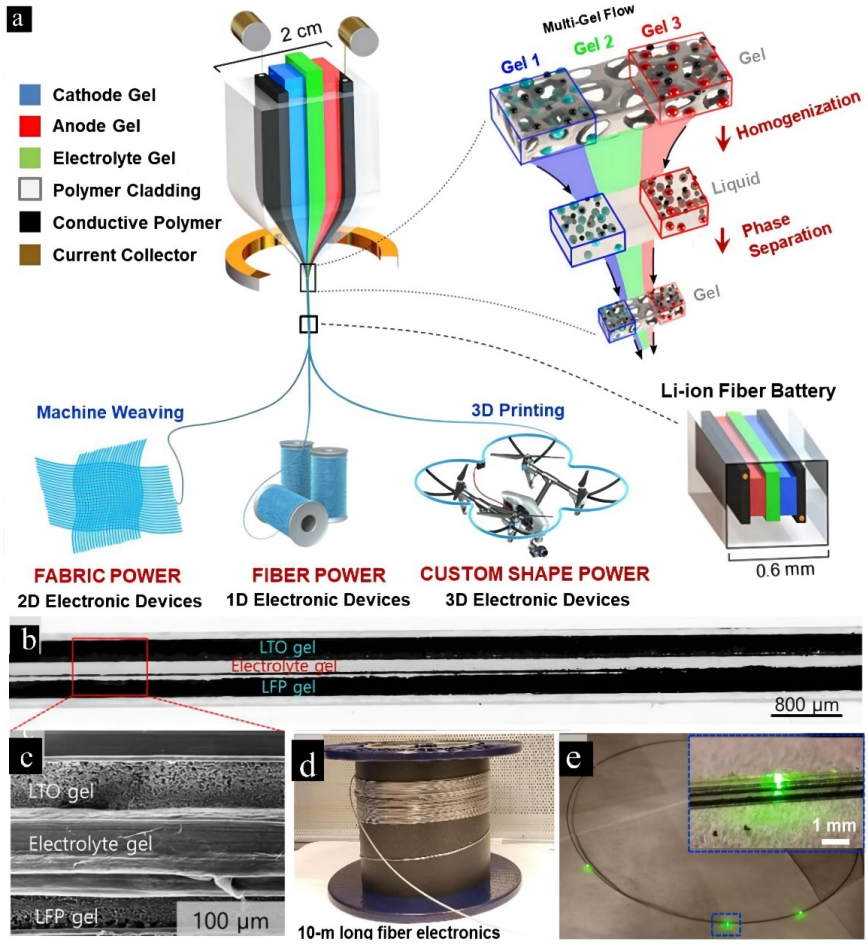


**Figure 5.** (**a**) Configuration schematic of fiber-shaped batteries. (**b**) Image of the electrode cross-section. (**c**) SEM image of the fiber-shaped battery. (**d**) A 10 m LED/battery fiber. (**e**) LEDs lit by fiber battery. Reprinted with permission from [51]. Copyright Elsevier Publisher, 2022.

Generally, the structures of fiber-shaped LIBs are mainly of two types: twisting LIBs and coaxial LIBs [52–56]. For twisting LIBs, the two electrodes are intertwined together to form a double-helix structure. For coaxial LIBs, one fiber electrode is selected as the core,

and the other wraps around the inner core to form a core-shell construct. Both types should avoid short circuit of the two opposite electrodes, so a separator is often employed when the electrolyte is liquid. For preparing flexible fiber-shaped LIBs, the core step is to develop flexible fiber electrodes with excellent conductivity and mechanical stability. Recently, flexible fiber-shaped electrodes have usually been obtained by compounding active materials onto the conductive fiber substrates. Various carbon materials have been developed and worked as substrates to support active materials and current collectors to transport electrons owing to their porosity, stability, large surface area and excellent conductivity.

Much research has demonstrated carbon-based composites as electrodes for FLIBs. Man et al. assembled flexible twisting LIBs [57], which were composed of a $LiCoO_2$ nanosheet array cathode (LCO@CNTF), ball-shaped $NaTi_2(PO_4)_3$ on CNT fiber anode (NTP@CNTF) and saturated $Li_2SO_4$ solution electrolyte, as illustrated in Figure 6a. The battery capacity retention was up to 94.74% after 3000 cycles at 90° bending (Figure 6b). Moreover, the batteries were integrated in series to light an LED under bending states (Figure 6c). They were assembled into a textile and powered the LED (Figure 6d), which demonstrated great potential application for flexible fiber-shaped batteries. Song et al. fabricated a coaxial fiber-shaped LIB with a length and diameter of 9 cm and 0.91 mm, respectively. It consisted of cotton as the core, wrapped CNT films as electrodes and a PVDF film as a separator (Figure 6e–h) [58]. The cotton fiber exhibited high mechanical strength (with stress in the axial and circumferential directions up to 86.8 KPa and 67.4 KPa, respectively (Figure 6i)) and superior charge and discharge performance (Figure 6j). Moreover, the fiber battery was put into practical application (Figure 6k,l), which showed the great potential of the fiber-shaped batteries as flexible energy storage devices.

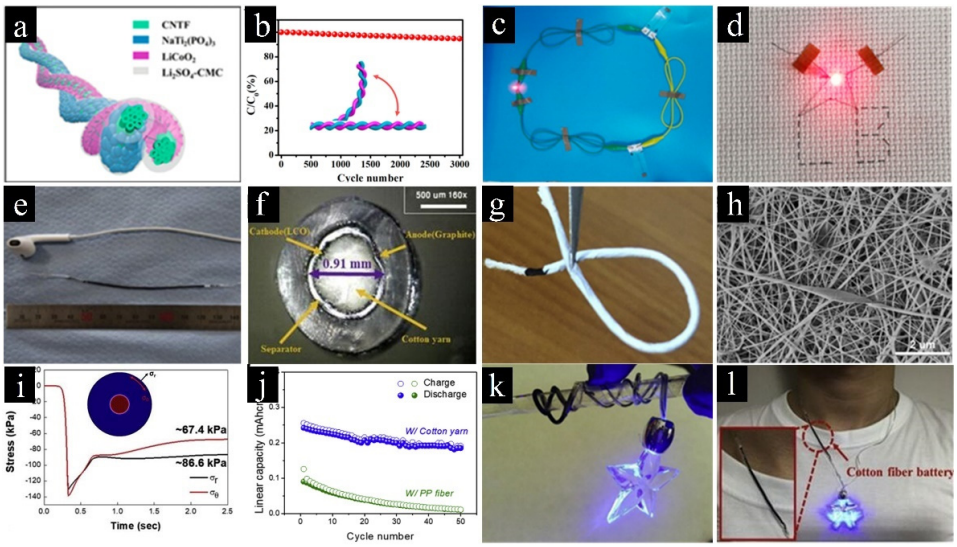


**Figure 6.** (**a**) Schematic of the assembled twisting LIB. (**b**) Cycle stability at 90° bending of the LIB. Images of (**c**) the LIBs in series lighting an LED, and (**d**) the LED powered by the LIB textile. (**a**–**d**) Reprinted with permission from [57]. Copyright American Chemical Society Publisher, 2020. (**e**) Image of the 9 cm fiber battery. (**f**) Cross-section of the as-assembled fiber-shaped battery. (**g**) Image of a PVDF separator coated on the electrode. (**h**) SEM image of the PVDF film. (**i**) The development of stress in the fiber surface during expansion. (**j**) Cycle stability comparison of cotton fiber battery and polypropylene fiber battery. (**k**,**l**) Images of the as-assembled fiber battery application. (**e**–**l**) Reprinted with permission from [58]. Copyright Elsevier Publisher, 2019.

As mentioned above, carbon materials have been widely investigated by testing diverse fiber-shaped batteries. The as-assembled batteries show unique superiority and could be integrated into flexible electronics [53,54]. With carbon material optimization and structure design improvement, the high specific capacity and cycling life of batteries will play an indispensable role in implantable and wearable electronics. We comprehensively

summarize the performances of some fiber-shaped FLIBs reported recently, as shown in Table 1.

**Table 1.** The performance of reported 1D fiber-shaped FLIBs.

| Carbon-Based Electrodes | Specific Capacity | Current Density | Cycling Life | Capacity Retention | Reference |
|---|---|---|---|---|---|
| $SnO_2$@rGO/$LiCoO_2$@rGO | 82.6 mAh $g^{-1}$ | 0.1 A $g^{-1}$ | | | [59] |
| LTP@CNT/LFP@CNT | 29.1 mAh $g^{-1}$ | 0.25 A $g^{-1}$ | | | [60] |
| graphite/LCO | 170 mAh $g^{-1}$ | 0.017 A $g^{-1}$ | 500 | 93% | [61] |
| graphite@CNT/$LiNi_{0.6}Co_{0.2}Mn_{0.2}O_2$@CNT | 166 mAh $g^{-1}$ | 0.1C | 50 | 99% | [53] |
| NTP@CNT/LCO@CNT | 45.2 mAh $cm^{-3}$ | 0.2 A $cm^{-3}$ | 3000 | 94.7% | [57] |
| graphite@CNT/LCO@CNT | 141.8 mAh $g^{-1}$ | 0.145 A $g^{-1}$ | 50 | 84% | [58] |
| $TiO_2$@rGO/$LiMn_2O_4$ | 126 mAh $g^{-1}$ | 0.017 mA $g^{-1}$ | 100 | 80% | [62] |
| LTO@CNT/LCO@CNT | 135 mAh $g^{-1}$ | 0.15 A $g^{-1}$ | 100 | 86.2% | [63] |
| Ag@rGo/$MnO_2$@rGO | 24.5 mF $cm^{-2}$ | 0.1 mA $cm^{-2}$ | 3000 | 94.3% | [64] |
| CNT@$Fe_2O_3$/CNT@NiO@$MnO_x$ | 10.4 F·$cm^{-3}$ | 30 mA $cm^{-3}$ | 2000 | 95% | [65] |
| Graphene fibers | 973.1 mF $cm^{-3}$ | 161.6 mA $cm^{-3}$ | 10,000 | 91% | [66] |
| CNT/$MnO_2$@CF | 91.6 F $cm^{-3}$ | 104.7 mA $cm^{-3}$ | 7000 | 95.3% | [67] |

### *3.2. 2D Paper-like Batteries*

The conventional LIBs are fabricated by coating slurry composed of active materials, conductive materials and binders layer by layer on metal foils, which results in the LIBs being rigid and heavy. In addition, the active materials of electrodes fabricated by the slurry-casting strategy are apt to detach from the metal foils when the batteries suffer bending/stretching and releasing periodically, lowering the flexibility and reliability of LIBs.

Flexible freestanding electrodes without binders and metal foils make them light and avoid detaching problems [68–71]. Carbon-based materials, such as CNTs and graphene, are the most popular flexible electrode materials owing to their diverse structure, facile synthesis process and excellent physical and electrochemical stability. Numerous efforts have been promoted to prepare freestanding electrodes based on carbon-based materials.

For fabricating freestanding electrodes of paper-like batteries, the carbon-based macroscopic films often serve as current collectors to let active materials grow on the surfaces [72–76]. For example, Wei et al. synthesized flexible and foldable CNT films, as shown in Figure 7a, using the floating catalyst CVD method [77]. The as-fabricated CNT films with a width of 1 m can replace metal foil and be employed to achieve the production of flexible LIBs on a large scale. Figure 7c,d show the flexibility comparison for LCO coated on Al foil and CNT film, which demonstrated that the porous and rough CNT film is conducive to increasing the contact surface and adhesion significantly. Then, they used $LiCoO_2$ (LCO) as the positive electrode and $Li_4Ti_5O_{12}$ (LTO) as the negative electrode to form a flexible full cell for the performance test. Unlike conventional coin cells, which are rigid and intolerant to deformation, the as-fabricated cell could be tailored to various shapes to adapt to highly integrated and wearable environments. The unpackaged device could still power an LED after several cycles of folding and punching (Figure 7e–i). Notably, the open-circuit voltage of the cell remained at 2.34 V, over 92.8% of the initial value (Figure 7j), which demonstrated an ignorable current leakage during deformation. The results indicated that the as-fabricated cell could be employed as a tailorable and deformable energy storage device for implantable and wearable electronics.

Electrospinning is a popular approach for preparing freestanding electrodes [78–82]. For example, Zhang et al. prepared a freestanding and foldable composite electrode with active material ZnSe assembled in a CNF network (Figure 7k,l) by an electrospinning and subsequent carbonization/selenization strategy [83]. The HRTEM image (Figure 7m), TEM image (Figure 7n) and elemental mapping images (Figure 7o–q) show the morphological

characteristics and composition of ZnSe@CNFs. The as-fabricated FLIB exhibited high specific capacity and long cycling life (Figure 7w). For further application, a pouch battery lit the LEDs. Even though it suffered repeated folding at various angles, it was in accordance with the original statement (Figure 7r–v). The superior FLIB confirmed that the design was conducive to promoting the prosperous development of freestanding electrodes for wearable electronics.

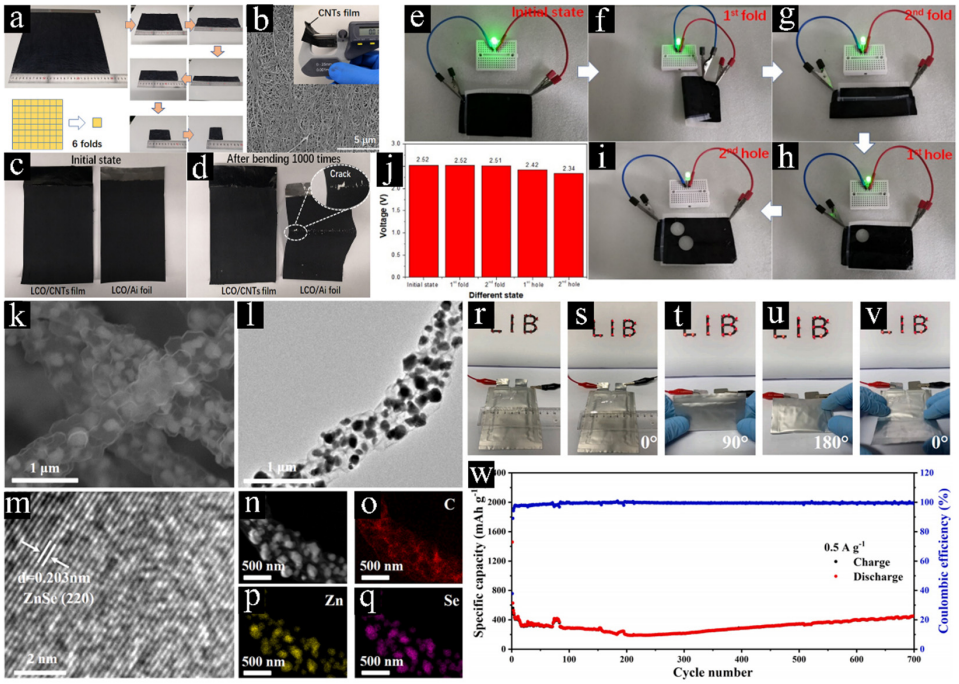


**Figure 7.** (**a**) Folding process and (**b**) SEM image of the CNT film. Images of LCO/CNT film and LCO/Ai foil (**c**) before and (**d**) after bending 1000 cycles. Flexible test of the battery: (**e**) Initial state. (**f**) After 1st fold. (**g**) After 2nd fold. (**h**) After 1st punch. (**i**) After 2nd punch. (**j**) Voltages under different statuses. (**a**–**j**) Reprinted with permission from [77]. Copyright Elsevier Publisher, 2022. (**k**) SEM, (**l**) TEM, (**m**) HRTEM and (**n**–**q**) Annular dark-filed TEM image of ZnSe@CNFs-2.5. Qualitative test of the pouch cell by power LEDs under various deformations: (**r**) Pristine, (**s**) 0°, (**t**) 90°, (**u**) 180°, (**v**) back to 0°. (**w**) Cycling stability of the cell. (**k**–**w**) Reprinted with permission from [83]. Copyright Elsevier Publisher, 2022.

There are many approaches for forming freestanding electrodes, such as composing carbon materials with active materials to develop solutions and then forming composite films by vacuum filtration. In addition, by electrodeposition, the active materials can also be deposited onto the carbon substrates. High mass loading of the active materials on carbon-based substrates with excellent conductivity and binder-free properties will contribute to a considerable energy density for the as-fabricated FLIBs.

### *3.3. Interdigital Batteries*

The ever-increasing boom in wearable and miniature electronic devices has accelerated the demand for on-chip power units. The above-mentioned paper-like FLIBs have shown advanced performance both in mechanical and electrochemical properties. However, the thickness, size and weight of paper-like FLIBs are still far from those required for miniature electronics. Miniature power source system technology is of great importance to reduce the size of units because the battery occupies 85% of the total weight and 35% of the volume [84]. This propels the development of high-performance microbatteries, such as micro-FLIBs.

The most popular micro-FLIBs are the units with on-chip interdigital structures, which are widely adopted in microsupercapacitors (MSCs). As all the components, such as anode, cathode and the solid electrolyte, are on a uniform substrate, MSCs are ideal candidates

for self-powered integrated microelectronic systems. Recently, advanced 3D printing technologies [85–91], such as direct ink writing, inkjet printing and stereolithography, have been widely used for the preparation of miniature electrodes with complex microstructures for interdigital FLIBs. Recently, Zheng et al. prepared interesting all-solid-state planar lithium-ion microcapacitors (LIMCs) [92]. The LIMCs were assembled by layer-upon-layer mask-assisted deposition on an interdigital film with carbon-coated $Li_4Ti_5O_{12}$ (LTO) as the negative electrode, activated graphene (AG) as the positive electrode and ion gel as the solid electrolyte (Figure 8a). The as-assembled LIMCs demonstrated high flexibility and could be assembled in series to obtain microcapacitor patterns (Figure 8b–h). The volumetric energy density of the as-assembled LIMCs is as high as 53.5 mWh $cm^{-3}$. In addition, they exhibited excellent mechanical flexibility and stable electrochemical performance even if under repeated bending (Figure 8i–k). The microdevice revealed outstanding modular integration for boosting voltage and capacitance (Figure 8l), which indicated LIMCs have great potential for application in miniature electronic devices.

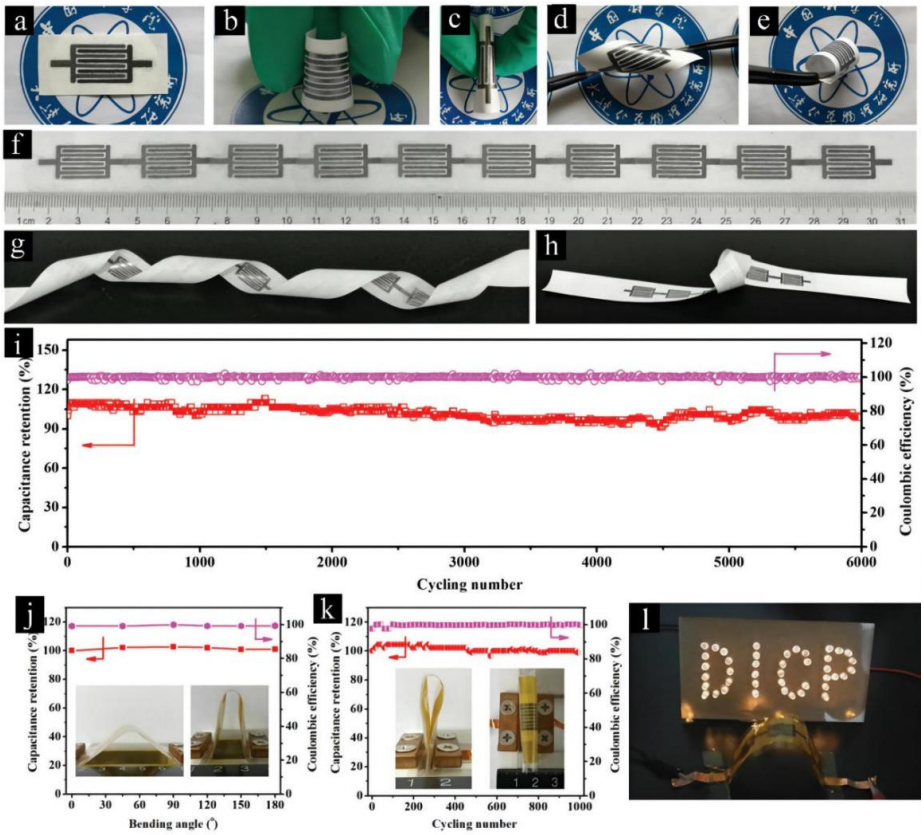


**Figure 8.** (**a**–**h**) Images of LIMCs (in series) in flat, bending, twisted and circled, spiral and knotted states. (**i**) Cycling stability of LIMCs for 6000 cycles. (**j**) Capacitance retention as a function of the bending angles. (**k**) Cycling stability in the state of a circle shape. (**l**) Images of the DICP logo powered by three in-series LIMCs under bending. Reprinted with permission from [92]. Copyright Elsevier Publisher, 2022.

The preparation of active materials and microelectrode pattern and then modular integration to form MSCs were originally separated and included several complicated steps. To date, laser processing technologies have greatly boosted the design ability and manufacturing accuracy of the microstructure [93–97]. Shi et al. reported a one-step method for scalable preparation of patterned laser-induced graphene (LIG), which acted as both microelectrode and conductive interconnector for planar integrated MSCs (LIG-MSCs) with designable shapes [98]. The areal capacitance of the as-fabricated LIG-MSCs is as high as 0.62 mF $cm^{-2}$ and they have excellent cycling stability (no capacitance degeneration after

10,000 cycles). Moreover, the LIG-MSCs demonstrated outstanding flexibility, adjustable voltage and capacitance output through arbitrary arrangements such as in series and parallel, indicative of exceptional performance customization.

### *3.4. Stretchable Batteries*

Stretchable electronic devices are employed as soft electronic devices, which may not only be bent, but also be stretched, deformed and wrapped on non-planar surfaces in conditions that cannot be tolerated by original flexible electronic devices [99–101]. Recently, numerous efforts have been promoted to develop stretchable energy storage devices to overcome the weakness of flexible energy storage devices. Generally speaking, there are two ways to achieve stretchability. One is creating special bulked structure designs for originally rigid devices, such as origami, wave and helically coiled spring structures, which are structurally stretchable. The other is replacing rigid components with stretchable ones, such as active electrodes, electrolytes, separators and packagings, which are intrinsically stretchable. For instance, using an elastic electrolyte to replace liquid electrolyte could provide better stretchability and safety while maintaining similar electrochemical performance.

Combined structurally stretchable and intrinsically stretchable designs achieves superior performance. Qian et al. dispersed CNTs and active materials in water with the assistance of nanofibrillated cellulose to form stable uniform aqueous ink for 3D extrusion-based printing [102], as shown in Figure 9a,d. The as-fabricated electrodes and separators could accomplish reversible stretchability as high as 50% (Figure 9e). After 50 cycles, the resistance of the stretchable electrode only increased by 3% (Figure 9b). Owing to the well-maintained structure of the electrode, the anode possessed specific capacity of 355 mAh $g^{-1}$ after 100 discharge-charge cycles (Figure 9c). The results demonstrated great potential to enable stretchable batteries for wearable and epidermal electronic devices.

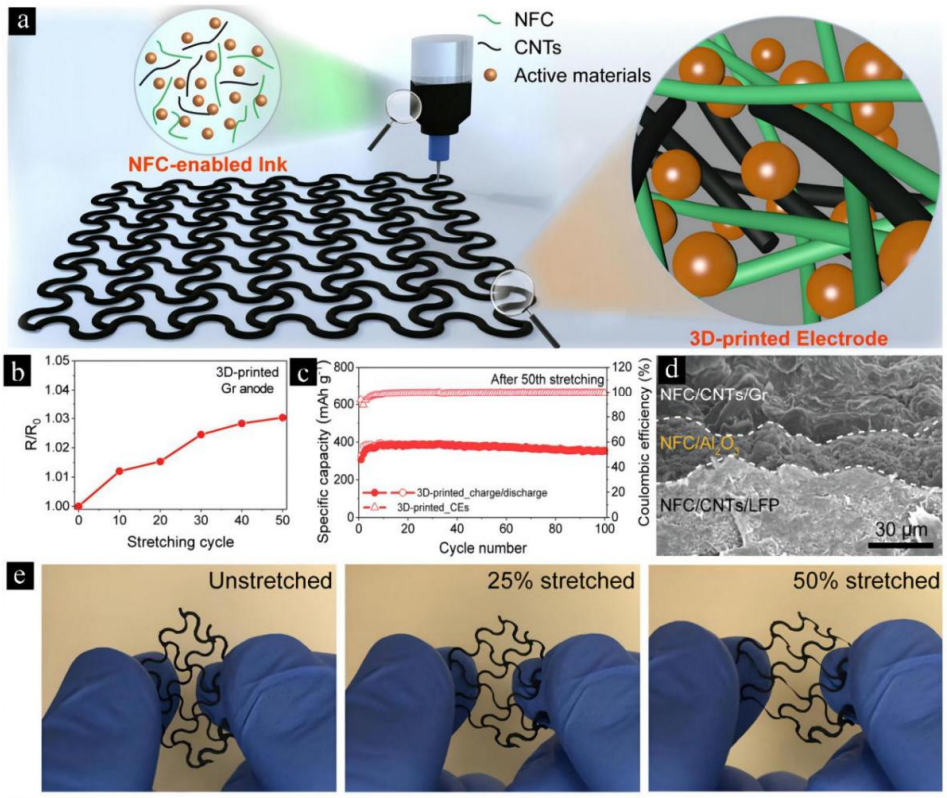


**Figure 9.** (**a**) Composition and morphology of the ink for 3D printing. (**b**) Normalized resistance after different cycles. (**c**) Cycling stability of the electrode after 50th stretching. (**d**) SEM image of cross-section for the electrodes and separator. (**e**) Images of the electrode in different stretched states. Reprinted with permission from [102]. Copyright Elsevier Publisher, 2022.

## 4. Conclusions and Prospects

In conclusion, we have investigated the most recent achievements in the novel design and controlled fabrication of various carbon materials, including CNTs, CNFs, graphene, GDY, CAs, etc., for FLIBs with fiber-shaped, paper-like, interdigital and stretchable structures. There are unique superiorities of carbon materials applied in flexible batteries. (1) Carbon materials with porous and large surfaces can provide a robust and conductive cross-linked framework for active materials to adhere firmly. In addition, the carbon framework can accommodate repeated deformation and allows both ion and electron transportation, efficiently enhancing electrochemical kinetics. (2) Excellent properties of carbon materials, such as light weight, low interface resistance and abundant active sites, are conducive to increasing the energy density of FLIBs. (3) Outstanding electrochemical stability of carbon materials enhances rate capability and favorable cyclic reversibility of the electrodes for FLIBs.

Numerous achievements and breakthrough progress have been promoted for carbon-based anode materials of FLIBs in the past few years, but there are still the following difficulties and challenges that hinder their development and application: the specific capacity is still low, compared to the theoretical capacity; the capacity fades fast after cyclic deformations; the mass of loaded active materials on carbon-based electrodes is limited, which is not conducive to volumetric/area energy densities; there are rarely strategies and devices for large-scale and reproducible synthesis of carbon materials with desired structures and morphologies at low cost. Therefore, developing flexible carbon-based anode materials with excellent flexibility, high energy capacity, large-scale production and low cost will be the main research direction in the future.

It is confirmed that carbon-based materials are one of the most favorable electrode materials for FLIBs. However, there is still a long way to go to overcome the current difficulties to meet the requirements of intelligent flexible and wearable electronics. We firmly believe that in the future, FLIBs combining outstanding mechanical flexibility and electrochemical performance will contribute to great advances in energy storage technology and boost the development and commercialization of portable and flexible electronics, given tremendous progress in structure design technology and material synthesis engineering.

**Author Contributions:** L.D. and T.W.: original draft preparation; T.W. and J.C.: review and editing; L.D. and J.L.: formatting and graphics; L.D., L.Z. and W.C.: funding acquisition. All authors have read and agreed to the published version of the manuscript.

**Funding:** This work is supported by the Guangdong Basic and Applied Basic Research Foundation (No.2021A1515110347) and Natural Science Foundation of Hunan Province (No.2022JJ40447) and Hunan Provincial Education Office Foundation of China (No.21B0146, 21C0086).

**Conflicts of Interest:** The authors declare that there are no conflict of interest regarding the publication of this manuscript.

## References

1. Wu, Z.; Wang, Y.; Liu, X.; Lv, C.; Li, Y.; Wei, D.; Liu, Z. Carbon-Nanomaterial-Based Flexible Batteries for Wearable Electronics. *Adv. Mater.* **2019**, *31*, 1800716. [CrossRef] [PubMed]
2. Khan, S.; Ul-Islam, M.; Ahmad, M.W.; Khan, M.S.; Imran, M.; Siyal, S.H.; Javed, M.S. Synthetic Methodologies and Energy Storage/Conversion Applications of Porous Carbon Nanosheets: A Systematic Review. *Energy Fuels* **2022**, *36*, 3420–3442. [CrossRef]
3. Zheng, Z.; Xue, Y.; Li, Y. A new carbon allotrope: Graphdiyne. *Trends Chem.* **2022**, *4*, 754–768. [CrossRef]
4. Salah, L.S.; Ouslimani, N.; Bousba, D.; Huynen, I.; Danlée, Y.; Aksas, H. Carbon Nanotubes (CNTs) from Synthesis to Functionalized (CNTs) Using Conventional and New Chemical Approaches. *J. Nanomater.* **2021**, *2021*, 4972770. [CrossRef]
5. Rathinavel, S.; Priyadharshini, K.; Panda, D. A review on carbon nanotube: An overview of synthesis, properties, functionalization, characterization, and the application. *Mater. Sci. Eng. B* **2021**, *268*, 115095. [CrossRef]
6. Shi, S.; Wang, G.; Wan, G.; Tang, Y.; Zhao, G.; Deng, Z.; Chai, J.; Wei, C.; Wang, G. Titanium niobate ($Ti_2Nb_{10}O_{29}$) anchored on nitrogen-doped carbon foams as flexible and self-supported anode for high-performance lithium ion batteries. *J. Colloid Interface Sci.* **2021**, *587*, 622–632. [CrossRef]

7. Zhao, M.; Xia, Y.; Mei, L. Diffusion and condensation of lithium atoms in single-walled carbon nanotubes. *Phys. Rev. B* **2005**, *71*, 165413. [CrossRef]
8. Huang, L.; Guan, Q.; Cheng, J.; Li, C.; Ni, W.; Wang, Z.; Zhang, Y.; Wang, B. Free-standing N-doped carbon nanofibers/carbon nanotubes hybrid film for flexible, robust half and full lithium-ion batteries. *Chem. Eng. J.* **2018**, *334*, 682–690. [CrossRef]
9. Sun, N.; Wang, X.; Dong, X.; Huang, H.; Qi, M. PVP-grafted synthesis for uniform electrospinning silica@carbon nanofibers as flexible free-standing anode for Li-ion batteries. *Solid State Ion.* **2021**, *374*, 115817. [CrossRef]
10. Zhang, M.; Li, L.; Jian, X.; Zhang, S.; Shang, Y.; Xu, T.; Dai, S.; Xu, J.; Kong, D.; Wang, Y.; et al. Free-standing and flexible CNT/(Fe@Si@$SiO_2$) composite anodes with kernel-pulp-skin nanostructure for high-performance lithium-ion batteries. *J. Alloys Compd.* **2021**, *878*, 160396. [CrossRef]
11. Yu, H.; Chen, L.; Li, W.; Dirican, M.; Liu, Y.; Zhang, X. Root-whisker structured 3D CNTs-CNFs network based on coaxial electrospinning: A free-standing anode in lithium-ion batteries. *J. Alloys Compd.* **2021**, *863*, 158481. [CrossRef]
12. Wang, B.; Xia, Y.; Deng, Z.; Zhang, Y.; Wu, H. Three-dimensional cross-linked MnO/Sb hybrid nanowires co-embedded nitrogen-doped carbon tubes as high-performance anode materials for lithium-ion batteries. *J. Alloys Compd.* **2020**, *835*, 155239. [CrossRef]
13. Yang, X.; Wu, L.; Hou, J.; Meng, B.; Ali, R.; Liu, Y.; Jian, X. Symmetrical growth of carbon nanotube arrays on FeSiAl micro-flake for enhancement of lithium-ion battery capacity. *Carbon* **2022**, *189*, 93–103. [CrossRef]
14. Wang, M.-S.; Wang, Z.-Q.; Chen, Z.; Yang, Z.-L.; Tang, Z.-L.; Luo, H.-Y.; Huang, Y.; Li, X.; Xu, W. One dimensional and coaxial polyaniline@tin dioxide@multi-wall carbon nanotube as advanced conductive additive free anode for lithium ion battery. *Chem. Eng. J.* **2018**, *334*, 162–171. [CrossRef]
15. Guo, W.; Si, W.; Zhang, T.; Han, Y.; Wang, L.; Zhou, Z.; Lu, P.; Hou, F.; Liang, J. Ultrathin $Ni_xCo_y$-silicate nanosheets natively anchored on CNTs films for flexible lithium ion batteries. *J. Energy Chem.* **2021**, *54*, 746–753. [CrossRef]
16. Liang, P.; Zhu, K.; Rao, Y.; Zheng, H.; Yao, Z.; Wu, M.; Zhang, J.; Liu, J.; Yan, K.; Wang, J.; et al. Flexible and Self-Standing Urchinlike $V_2O_3$@Carbon Nanofibers toward Ultralong Cycle Lifespan Lithium-Ion Batteries. *ACS Appl. Energy Mater.* **2022**, *5*, 3242–3251. [CrossRef]
17. Liu, Y.; Bai, M.; Du, D.; Tang, X.; Wang, H.; Zhang, M.; Zhao, T.; Liu, F.; Wang, Z.; Ma, Y. Affinity-Engineered Flexible Scaffold toward Energy-Dense, Highly Reversible Na Metal Batteries. *Energy Environ. Mater.* **2022**. [CrossRef]
18. Joshi, B.; Samuel, E.; Kim, Y.-I.; Yarin, A.L.; Swihart, M.T.; Yoon, S.S. Progress and potential of electrospinning-derived substrate-free and binder-free lithium-ion battery electrodes. *Chem. Eng. J.* **2022**, *430*, 132876. [CrossRef]
19. Gao, M.; Liu, B.; Zhang, X.; Zhang, Y.; Li, X.; Han, G. Ultrathin MoS2 nanosheets anchored on carbon nanofibers as free-standing flexible anode with stable lithium storage performance. *J. Alloys Compd.* **2021**, *894*, 162550. [CrossRef]
20. Zhou, X.-H.; Gao, Y.; Lyu, L.-H.; Liang, Y.-Y.; Li, Z.-H. General construction of molybdenum-based compounds embedded in flexible 3D interconnected porous carbon nanofibers with protective porous shell for high-performance lithium-ion battery. *Carbon* **2021**, *179*, 142–150. [CrossRef]
21. Zhu, J.; Wu, Y.; Huang, X.; Huang, L.; Cao, M.; Song, G.; Guo, X.; Sui, X.; Ren, R.; Chen, J. Self-healing liquid metal nanoparticles encapsulated in hollow carbon fibers as a free-standing anode for lithium-ion batteries. *Nano Energy.* **2019**, *62*, 883–889. [CrossRef]
22. Yadav, A.; De, B.; Singh, S.K.; Sinha, P.; Kar, K.K. Facile Development Strategy of a Single Carbon-Fiber-Based All-Solid-State Flexible Lithium-Ion Battery for Wearable Electronics. *ACS Appl. Mater. Interfaces* **2019**, *11*, 7974–7980. [CrossRef] [PubMed]
23. Wang, S.-G.; Lin, J.; Fan, C.-Y.; Li, Y.-F.; Zhang, J.-P.; Wu, X.-L.; Sun, H.-Z.; Deng, M.-X.; Su, Z.-M. Target encapsulating $NiMoO_4$ nanocrystals into 1D carbon nanofibers as free-standing anode material for lithium-ion batteries with enhanced cycle performance. *J. Alloys Compd.* **2020**, *830*, 154648. [CrossRef]
24. Yu, C.C.; Chen, Y.W.; Yeh, P.Y.; Hsiao, Y.S.; Lin, W.T.; Kuo, C.W.; Chueh, D.Y.; You, Y.W.; Shyue, J.J.; Chang, Y.C.; et al. Random and aligned electrospun PLGA nanofibers embedded in microfluidic chips for cancer cell isolation and integration with air foam technology for cell release. *J. Nanobiotechnol.* **2019**, *17*, 31. [CrossRef] [PubMed]
25. Li, J.; Zhang, W.; Zhang, X.; Huo, L.; Liang, J.; Wu, L.; Liu, Y.; Gao, J.; Pang, H.; Xue, H. Copolymer derived micro/meso-porous carbon nanofibers with vacancy-type defects for high-performance supercapacitors. *J. Mater. Chem. A* **2020**, *8*, 2463–2471. [CrossRef]
26. Wang, Y.; Li, J.; Li, X.; Jin, H.; Ali, W.; Song, Z.; Ding, S. Metal–organic-framework derived Co@CN modified horizontally aligned graphene oxide array as free-standing anode for lithium-ion batteries. *J. Mater. Chem. A* **2022**, *10*, 699–706. [CrossRef]
27. He, D.; Sun, M.; Cao, D.; Ding, Y.; Chen, H.; He, G. Flexible Free-Standing $Fe_2O_3$ Nanoparticle/Carbon Shells/Graphene Films for Advanced Lithium-Ion Batteries. *ACS Appl. Nano Mater.* **2022**, *5*, 5017–5024. [CrossRef]
28. Dai, C.; Sun, G.; Hu, L.; Xiao, Y.; Zhang, Z.; Qu, L. Recent progress in graphene-based electrodes for flexible batteries. *InfoMat* **2019**, *2*, 509–526. [CrossRef]
29. Zhai, S.; Wei, L.; Karahan, H.E.; Chen, X.; Wang, C.; Zhang, X.; Chen, J.; Wang, X.; Chen, Y. 2D materials for 1D electrochemical energy storage devices. *Energy Storage Mater.* **2019**, *19*, 102–123. [CrossRef]
30. Tang, P.; Deng, Z.; Zhang, Y.; Liu, L.X.; Wang, Z.; Yu, Z.Z.; Zhang, H.-B. Tough, Strong, and Conductive Graphene Fibers by Optimizing Surface Chemistry of Graphene Oxide Precursor. *Adv. Funct. Mater.* **2022**, *32*, 2112156. [CrossRef]
31. Mahmood, A.; Yuan, Z.; Sui, X.; Riaz, M.A.; Yu, Z.; Liu, C.; Chen, J.; Wang, C.; Zhao, S.; Mahmood, N.; et al. Foldable and scrollable graphene paper with tuned interlayer spacing as high areal capacity anodes for sodium-ion batteries. *Energy Storage Mater.* **2021**, *41*, 395–403. [CrossRef]

32. Liu, Y.; Fang, Y.; Zhao, Z.; Yuan, C.; Lou, X.W.D. A Ternary $Fe_{1-x}S$@Porous Carbon Nanowires/Reduced Graphene Oxide Hybrid Film Electrode with Superior Volumetric and Gravimetric Capacities for Flexible Sodium Ion Batteries. *Adv. Energy Mater.* **2019**, *9*, 1803052. [CrossRef]
33. Chen, X.; Jiang, X.; Yang, N. Graphdiyne Electrochemistry: Progress and Perspectives. *Small* **2022**, *18*, e2201135. [CrossRef] [PubMed]
34. Febrian, R.; Septiani, N.L.W.; Iqbal, M.; Yuliarto, B. Review—Recent Advances of Carbon-Based Nanocomposites as the Anode Materials for Lithium-Ion Batteries: Synthesis and Performance. *J. Electrochem. Soc.* **2021**, *168*, 110520. [CrossRef]
35. Kong, F.; Yue, Y.; Li, Q.; Ren, S. Sulfur-Doped Graphdiyne as a High-Capacity Anode Material for Lithium-Ion Batteries. *Nanomaterials* **2021**, *11*, 1161. [CrossRef] [PubMed]
36. Yang, Z.; Shen, X.; Wang, N.; He, J.; Li, X.; Wang, X.; Hou, Z.; Wang, K.; Gao, J.; Jiu, T.; et al. Graphdiyne Containing Atomically Precise N Atoms for Efficient Anchoring of Lithium Ion. *ACS Appl. Mater. Interfaces* **2019**, *11*, 2608–2617. [CrossRef]
37. Yang, H.-R.; Yang, Y.; Seo, H.; Kim, K.; Lee, H.S.; Lee, J.; Lee, J.; Kim, J.-H. SnS nanosheets on carbon foam as a flexible anode platform for rechargeable Li- and Na-ion batteries. *Appl. Surf. Sci.* **2021**, *544*, 148837. [CrossRef]
38. Wang, C.; Xiong, Y.; Wang, H.; Jin, C.; Sun, Q. Naturally three-dimensional laminated porous carbon network structured short nano-chains bridging nanospheres for energy storage. *J. Mater. Chem. A* **2017**, *5*, 15759–15770. [CrossRef]
39. Peydayesh, M.; Vogt, J.; Chen, X.; Zhou, J.; Donat, F.; Bagnani, M.; R. Müller, C.; Mezzenga, R. Amyloid-based carbon aerogels for water purification. *Chem. Eng. J.* **2022**, *449*, 137703. [CrossRef]
40. Inagaki, M.; Qiu, J.; Guo, Q. Carbon foam: Preparation and application. *Carbon* **2015**, *87*, 128–152. [CrossRef]
41. Huang, R.; Li, Y.; Song, Y.; Wang, L. Facial preparation of N-doped carbon foam supporting $Co_3O_4$ nanorod arrays as free-standing lithium-ion batteries' anode. *J. Alloys Compd.* **2019**, *818*, 152839. [CrossRef]
42. Wang, X.; Fei, S.; Huang, S.; Wu, C.; Zhao, J.; Chen, Z.; Uvdal, K.; Hu, Z. $MoS_2$ nanosheets inlaid in 3D fibrous N-doped carbon spheres for lithium-ion batteries and electrocatalytic hydrogen evolution reaction. *Carbon* **2019**, *150*, 363–370. [CrossRef]
43. Liu, W.; Fu, Y.; Li, Y.; Chen, S.; Song, Y.; Wang, L. Three-dimensional carbon foam surrounded by carbon nanotubes and Co-$Co_3O_4$ nanoparticles for stable lithium-ion batteries. *Compos. Part B Eng.* **2019**, *163*, 464–470. [CrossRef]
44. Yuan, W.; Wang, B.; Wu, H.; Xiang, M.; Wang, Q.; Liu, H.; Zhang, Y.; Liu, H.; Dou, S. A flexible 3D nitrogen-doped carbon foam@CNTs hybrid hosting $TiO_2$ nanoparticles as free-standing electrode for ultra-long cycling lithium-ion batteries. *J. Power Source* **2018**, *379*, 10–19. [CrossRef]
45. Liu, Z.; Bai, S.; Liu, B.; Guo, P.; Lv, M.; Liu, D.; He, D. Interfacial modification of a lightweight carbon foam current collector for high-energy density Si/LCO lithium-ion batteries. *J. Mater. Chem. A* **2017**, *5*, 13168–13175. [CrossRef]
46. Chen, J.; Wu, X.; Tan, Q.; Chen, Y. Designed synthesis of ultrafine NiO nanocrystals bonded on a three dimensional graphene framework for high-capacity lithium-ion batteries. *New J. Chem.* **2018**, *42*, 9901–9910. [CrossRef]
47. Sun, S.; Yan, Q.; Wu, M.; Zhao, X. Carbon aerogel based materials for secondary batteries. *Sustain. Mater. Technol.* **2021**, *30*, e00342. [CrossRef]
48. Zhang, S.; Feng, J.; Feng, J.; Jiang, Y.; Ding, F. Carbon aerogels by pyrolysis of TEMPO-oxidized cellulose. *Appl. Surf. Sci.* **2018**, *440*, 873–879. [CrossRef]
49. Guo, F.; Jiang, Y.; Xu, Z.; Xiao, Y.; Fang, B.; Liu, Y.; Gao, W.; Zhao, P.; Wang, H.; Gao, C. Highly stretchable carbon aerogels. *Nat. Commun.* **2018**, *9*, 881. [CrossRef]
50. Wang, Y.; Chen, C.; Xie, H.; Gao, T.; Yao, Y.; Pastel, G.; Han, X.; Li, Y.; Zhao, J.; Fu, K.; et al. 3D-Printed All-Fiber Li-Ion Battery toward Wearable Energy Storage. *Adv. Funct. Mater.* **2017**, *27*, 1703140. [CrossRef]
51. Khudiyev, T.; Grena, B.; Loke, G.; Hou, C.; Jang, H.; Lee, J.; Noel, G.; Alain, J.; Joannopoulos, J.; Li, K.; et al. Thermally drawn rechargeable battery fiber enables pervasive power. *Mater. Today* **2022**, *52*, 80–89. [CrossRef]
52. Praveen, S.; Sim, G.S.; Ho, C.W.; Lee, C.W. 3D-printed twisted yarn-type Li-ion battery towards smart fabrics. *Energy Storage Mater.* **2021**, *41*, 748–757. [CrossRef]
53. Ji, D.; Zheng, H.; Zhang, H.; Liu, W.; Ding, J. Coaxial 3D-printing constructing all-in-one fibrous lithium-, sodium-, and zinc-ion batteries. *Chem. Eng. J.* **2022**, *433*, 133815. [CrossRef]
54. Zhu, Y.H.; Yang, X.Y.; Liu, T.; Zhang, X.B. Flexible 1D Batteries: Recent Progress and Prospects. *Adv. Mater.* **2020**, *32*, e1901961. [CrossRef]
55. Zhou, Y.; Wang, C.H.; Lu, W.; Dai, L. Recent Advances in Fiber-Shaped Supercapacitors and Lithium-Ion Batteries. *Adv. Mater.* **2020**, *32*, e1902779. [CrossRef]
56. Qu, H.; Lu, X.; Skorobogatiy, M. All-Solid Flexible Fiber-Shaped Lithium Ion Batteries. *J. Electrochem. Soc.* **2018**, *165*, A688–A695. [CrossRef]
57. Man, P.; He, B.; Zhang, Q.; Li, C.; Zhou, Z.; Li, Q.; Xu, W.; Hong, G.; Yao, Y. High-Performance and Ultraflexible Aqueous Rechargeable Lithium-Ion Batteries Developed by Constructing All Binder-free Electrode Materials. *ACS Appl. Mater. Interfaces* **2020**, *12*, 25700–25708. [CrossRef]
58. Song, H.; Jeon, S.-Y.; Jeong, Y. Fabrication of a coaxial high performance fiber lithium-ion battery supported by a cotton yarn electrolyte reservoir. *Carbon* **2019**, *147*, 441–450. [CrossRef]
59. Rao, J.; Liu, N.; Zhang, Z.; Su, J.; Li, L.; Xiong, L.; Gao, Y. All-fiber-based quasi-solid-state lithium-ion battery towards wearable electronic devices with outstanding flexibility and self-healing ability. *Nano Energy* **2018**, *51*, 425–433. [CrossRef]

60. Zhang, T.; Han, S.; Guo, W.; Hou, F.; Liu, J.; Yan, X.; Chen, S.; Liang, J. Continuous carbon nanotube composite fibers for flexible aqueous lithium-ion batteries. *Sustain. Mater. Technol.* **2019**, *20*, e00096. [CrossRef]
61. He, J.; Lu, C.; Jiang, H.; Han, F.; Shi, X.; Wu, J.; Wang, L.; Chen, T.; Wang, J.; Zhang, Y.; et al. Scalable production of high-performing woven lithium-ion fiber batteries. *Nature* **2021**, *597*, 57–63. [CrossRef]
62. Hoshide, T.; Zheng, Y.; Hou, J.; Wang, Z.; Li, Q.; Zhao, Z.; Ma, R.; Sasaki, T.; Geng, F. Flexible Lithium-Ion Fiber Battery by the Regular Stacking of Two-Dimensional Titanium Oxide Nanosheets Hybridized with Reduced Graphene Oxide. *Nano Lett.* **2017**, *17*, 3543–3549. [CrossRef] [PubMed]
63. Wu, Z.; Liu, K.; Lv, C.; Zhong, S.; Wang, Q.; Liu, T.; Liu, X.; Yin, Y.; Hu, Y.; Wei, D.; et al. Ultrahigh-Energy Density Lithium-Ion Cable Battery Based on the Carbon-Nanotube Woven Macrofilms. *Small* **2018**, *14*, e1800414. [CrossRef] [PubMed]
64. Nguyen, P.T.; Jang, J.; Lee, Y.; Choi, S.T.; In, J.B. Laser-assisted fabrication of flexible monofilament fiber supercapacitors. *J. Mater. Chem. A* **2021**, *9*, 4841–4850. [CrossRef]
65. Yuan, H.; Wang, G.; Zhao, Y.; Liu, Y.; Wu, Y.; Zhang, Y. A stretchable, asymmetric, coaxial fiber-shaped supercapacitor for wearable electronics. *Nano Res.* **2020**, *13*, 1686–1692. [CrossRef]
66. Zhang, Z.; Zhang, D.; Lin, H.; Chen, Y. Flexible fiber-shaped supercapacitors with high energy density based on self-twisted graphene fibers. *J. Power Source* **2019**, *433*, 226711. [CrossRef]
67. Gong, W.; Fugetsu, B.; Wang, Z.; Ueki, T.; Sakata, I.; Ogata, H.; Han, F.; Li, M.; Su, L.; Zhang, X.; et al. Thicker carbon-nanotube/manganese-oxide hybridized nanostructures as electrodes for the creation of fiber-shaped high-energy-density supercapacitors. *Carbon* **2019**, *154*, 169–177. [CrossRef]
68. Xie, C.; Xu, N.; Shi, P.; Lv, Y.; Maleki Kheimeh Sari, H.; Shi, J.W.; Xiao, W.; Qin, J.; Yang, H.; Li, W.; et al. Flexible and robust silicon/carbon nanotube anodes exhibiting high areal capacities. *J. Colloid Interface Sci.* **2022**, *625*, 871–878. [CrossRef]
69. Kang, Y.; Deng, C.; Chen, Y.; Liu, X.; Liang, Z.; Li, T.; Hu, Q.; Zhao, Y. Binder-Free Electrodes and Their Application for Li-Ion Batteries. *Nanoscale Res. Lett.* **2020**, *15*, 112. [CrossRef]
70. Li, C.; Zhu, L.; Qi, S.; Ge, W.; Ma, W.; Zhao, Y.; Huang, R.; Xu, L.; Qian, Y. Ultrahigh-Areal-Capacity Battery Anodes Enabled by Free-Standing Vanadium Nitride@N-Doped Carbon/Graphene Architecture. *ACS Appl. Mater. Interfaces* **2020**, *12*, 49607–49616. [CrossRef]
71. Zhang, P.; Wang, F.; Yang, S.; Wang, G.; Yu, M.; Feng, X. Flexible in-plane micro-supercapacitors: Progresses and challenges in fabrication and applications. *Energy Storage Mater.* **2020**, *28*, 160–187. [CrossRef]
72. Zeng, Y.; Huang, Y.; Liu, N.; Wang, X.; Zhang, Y.; Guo, Y.; Wu, H.-H.; Chen, H.; Tang, X.; Zhang, Q. N-doped porous carbon nanofibers sheathed pumpkin-like Si/C composites as free-standing anodes for lithium-ion batteries. *J. Energy Chem.* **2021**, *54*, 727–735. [CrossRef]
73. Xia, J.; Zhang, X.; Yang, Y.; Wang, X.; Yao, J. Electrospinning fabrication of flexible, foldable, and twistable $Sb_2S_3/TiO_2/C$ nanofiber anode for lithium ion batteries. *Chem. Eng. J.* **2021**, *413*, 127400. [CrossRef]
74. Peng, J.; Tao, J.; Liu, Z.; Yang, Y.; Yu, L.; Zhang, M.; Wang, F.; Ding, Y. Ultra-stable and high capacity flexible lithium-ion batteries based on bimetallic MOFs derivatives aiming for wearable electronic devices. *Chem. Eng. J.* **2021**, *417*, 129200. [CrossRef]
75. Lian, X.; Xu, N.; Ma, Y.; Hu, F.; Wei, H.; Chen, H.-Y.; Wu, Y.; Li, L.; Peng, S. In-situ formation of $Co_{1-x}S$ hollow polyhedrons anchored on multichannel carbon nanofibers as self-supporting anode for lithium/sodium-ion batteries. *Chem. Eng. J.* **2020**, *421*, 127755. [CrossRef]
76. Li, X.; Deng, C.; Wang, H.; Si, J.; Zhang, S.; Huang, B. Iron Nitride@C Nanocubes Inside Core-Shell Fibers to Realize High Air-Stability, Ultralong Life, and Superior Lithium/Sodium Storages. *ACS Appl. Mater. Interfaces* **2021**, *13*, 7297–7307. [CrossRef] [PubMed]
77. Wei, D.; Shen, W.; Xu, T.; Li, K.; Yang, L.; Zhou, Y.; Zhong, M.; Yang, F.; Xu, X.; Wang, Y.; et al. Ultra-flexible and foldable gel polymer lithium–ion batteries enabling scalable production. *Mater. Today Energy* **2021**, *23*, 100889. [CrossRef]
78. Yang, Y.; Fu, W.; Bell, C.; Lee, D.C.; Drexler, M.; Nuli, Y.; Ma, Z.-F.; Magasinski, A.; Yushin, G.; Alamgir, F.S. Iron Phosphide Confined in Carbon Nanofibers as a Free-Standing Flexible Anode for High-Performance Lithium-Ion Batteries. *ACS Appl. Mater. Interfaces* **2021**, *13*, 34074–34083. [CrossRef]
79. Liu, J.; Liang, J.; Wang, C.; Ma, J. Electrospun CoSe@N-doped carbon nanofibers with highly capacitive Li storage. *J. Energy Chem.* **2019**, *33*, 160–166. [CrossRef]
80. Jiang, H.; Gan, Y.; Liu, J.; Wang, X.; Ma, R.; Liu, J.; Wang, J. Boosting the transport kinetics of free-standing $SnS_2$@Carbon nanofibers by electronic structure modulation for advanced lithium storage. *J. Mater. Chem. A* **2022**, *10*, 9468–9681. [CrossRef]
81. Zhu, R.; Wang, Z.; Hu, X.; Liu, X.; Wang, H. Silicon in Hollow Carbon Nanospheres Assembled Microspheres Cross-linked with N-doped Carbon Fibers toward a Binder Free, High Performance, and Flexible Anode for Lithium-Ion Batteries. *Adv. Funct. Mater.* **2021**, *31*, 2101487. [CrossRef]
82. Luiso, S.; Petrecca, M.J.; Williams, A.H.; Christopher, J.; Velev, O.D.; Pourdeyhimi, B.; Fedkiw, P.S. Structure-Performance Relationships of Li-Ion Battery Fiber-Based Separators. *ACS Appl. Polym. Mater.* **2022**, *4*, 3676–3686. [CrossRef]
83. Zhang, T.; Qiu, D.; Hou, Y. Free-standing and consecutive ZnSe@carbon nanofibers architectures as ultra-long lifespan anode for flexible lithium-ion batteries. *Nano Energy* **2022**, *94*, 106909. [CrossRef]
84. Li, B.; Yu, M.; Li, Z.; Yu, C.; Wang, H.; Li, Q. Constructing Flexible All-Solid-State Supercapacitors from 3D Nanosheets Active Bricks via 3D Manufacturing Technology: A Perspective Review. *Adv. Funct. Mater.* **2022**, *32*, 2201166. [CrossRef]

85. Jiang, X.; Gao, R.; Liu, G.; Luo, H.; Zhao, X.; Jiang, L. Construction of Graphene-Based "In-Paper" 3D Interdigital Microelectrodes for High Performance Metal-Free Flexible Supercapacitors. *Small Methods* **2022**, *6*, e2101454. [CrossRef]
86. Zhang, M.; Bai, R.; King, S.; Yin, F.; Peng, H.; Wang, G. Dual Active and Kinetically Inter-Promoting $Li_3VO_4$/Graphene Anode Enabling Printable High Energy Density Lithium Ion Micro Capacitors. *Energy Storage Mater.* **2021**, *43*, 482–491. [CrossRef]
87. Shi, X.; Tian, L.; Wang, S.; Wen, P.; Su, M.; Xiao, H.; Das, P.; Zhou, F.; Liu, Z.; Sun, C.; et al. Scalable and fast fabrication of graphene integrated micro-supercapacitors with remarkable volumetric capacitance and flexibility through continuous centrifugal coating. *J. Energy Chem.* **2021**, *52*, 284–290. [CrossRef]
88. Shi, X.; Pei, S.; Zhou, F.; Ren, W.; Cheng, H.-M.; Wu, Z.-S.; Bao, X. Ultrahigh-voltage integrated micro-supercapacitors with designable shapes and superior flexibility. *Energy Environ. Sci.* **2019**, *12*, 1534–1541. [CrossRef]
89. Zheng, S.; Wu, Z.-S.; Zhou, F.; Wang, X.; Ma, J.; Liu, C.; He, Y.-B.; Bao, X. All-solid-state planar integrated lithium ion micro-batteries with extraordinary flexibility and high-temperature performance. *Nano Energy* **2018**, *51*, 613–620. [CrossRef]
90. Liu, Y.; Zhang, B.; Xu, Q.; Hou, Y.; Seyedin, S.; Qin, S.; Wallace, G.; Beirne, B.; Razal, J.; Chen, J. Development of Graphene Oxide/Polyaniline Inks for High Performance Flexible Microsupercapacitors via Extrusion Printing. *Adv. Funct. Mater.* **2018**, *28*, 1706592. [CrossRef]
91. Chen, B.; Jiang, Y.; Tang, X.; Pan, Y.; Hu, S. Fully Packaged Carbon Nanotube Supercapacitors by Direct Ink Writing on Flexible Substrates. *ACS Appl. Mater. Interfaces* **2017**, *9*, 28433–28440. [CrossRef]
92. Zheng, S.; Ma, J.; Wu, Z.-S.; Zhou, F.; He, Y.-B.; Kang, F.; Cheng, H.-M.; Bao, X. All-solid-state flexible planar lithium ion micro-capacitors. *Energy Environ. Sci.* **2018**, *11*, 2001–2009. [CrossRef]
93. Ye, J.; Tan, H.; Wu, S.; Ni, K.; Pan, F.; Liu, J.; Tao, Z.; Qu, Y.; Ji, H.; Simon, P.; et al. Direct Laser Writing of Graphene Made from Chemical Vapor Deposition for Flexible, Integratable Micro-Supercapacitors with Ultrahigh Power Output. *Adv. Mater.* **2018**, *30*, e1801384. [CrossRef] [PubMed]
94. Lin, N.; Chen, H.; Wang, W.; Lu, L. Laser-Induced Graphene/$MoO_2$ Core-Shell Electrodes on Carbon Cloth for Integrated, High-Voltage, and In-Planar Microsupercapacitors. *Adv. Mater. Technol.* **2021**, *6*, 2000991. [CrossRef]
95. Liu, Y.; Wang, Y.; Meng, Y.; Plamthottam, R.; Tjiu, W.W.; Zhang, C.; Liu, T. Ultrathin Polypyrrole Layers Boosting $MoO_3$ as Both Cathode and Anode Materials for a 2.0 V High-Volt. Aqueous Supercapacitor. *ACS Appl. Mater. Interfaces* **2022**, *14*, 4490–4499. [CrossRef] [PubMed]
96. Zhang, W.; Li, R.; Zheng, H.; Bao, J.; Tang, Y.; Zhou, K. Laser-Assisted Printing of Electrodes Using Metal–Organic Frameworks for Micro-Supercapacitors. *Adv. Funct. Mater.* **2021**, *31*, 2009057. [CrossRef]
97. Li, Q.; Wang, Q.; Li, L.; Yang, L.; Wang, Y.; Wang, X.; Fang, H.-T. Femtosecond Laser-Etched MXene Microsupercapacitors with Double-Side Configuration via Arbitrary On- and Through-Substrate Connections. *Adv. Energy Mater.* **2020**, *10*, 2000470. [CrossRef]
98. Shi, X.; Zhou, F.; Peng, J.; Wu, R.; Wu, Z.S.; Bao, X. One-Step Scalable Fabrication of Graphene-Integrated Micro-Supercapacitors with Remarkable Flexibility and Exceptional Performance Uniformity. *Adv. Funct. Mater.* **2019**, *29*, 1902860. [CrossRef]
99. Hong, S.Y.; Jee, S.M.; Ko, Y.; Cho, J.; Lee, K.H.; Yeom, B.; Kim, H.; Son, J.G. Intrinsically Stretchable and Printable Lithium-Ion Battery for Free-Form Configuration. *ACS Nano* **2022**, *16*, 2271–2281. [CrossRef]
100. Chen, D.; Lou, Z.; Jiang, K.; Shen, G. Device Configurations and Future Prospects of Flexible/Stretchable Lithium-Ion Batteries. *Adv. Funct. Mater.* **2018**, *28*, 1805596. [CrossRef]
101. Song, W.-J.; Lee, S.; Song, G.; Park, S. Stretchable Aqueous Batteries: Progress and Prospects. *ACS Energy Lett.* **2018**, *4*, 177–186. [CrossRef]
102. Qian, J.; Chen, Q.; Hong, M.; Xie, W.; Jing, S.; Bao, Y.; Chen, G.; Pang, Z.; Hu, L.; Li, T. Toward stretchable batteries: 3D-printed deformable electrodes and separator enabled by nanocellulose. *Mater. Today* **2022**, *54*, 18–26. [CrossRef]